North Pacific Atmospheric and SST Anomalies in 1997: Links to ENSO?

JAMES E. OVERLAND[1,*], NICHOLAS A. BOND[2] AND JENNIFER MILETTA ADAMS[2]

[1]*NOAA, Pacific Marine Environmental Laboratory, Seattle, WA 98115, USA*
[2]*University of Washington, JISAO, Seattle, WA 98195, USA*

ABSTRACT

In the summer of 1997, positive sea surface temperature anomalies (SSTA) extended across the Gulf of Alaska (GOA) and into the eastern Bering Sea (EBS). The SSTA in the EBS are at least in part due to atmospheric causes. Anomalously high 925 mb temperatures and 700 mb geopotential heights and low 925 mb relative humidities, and hence decreased low cloud cover, occurred over the region during April to August. This resulted in enhanced warming of the GOA and EBS owing to increased insolation. The anomalous solar heating was particularly great in the EBS from mid-May to mid-July. The pattern of positive 700 mb height anomalies for April to August 1997 is similar to its counterpart formed by compositing the April to August anomalies that occurred during previous El Niños. The positive equatorial SSTA for 1997 was one of the strongest on record for summer months. The existence of an equatorial/high-latitude connection and the strength of the summer equatorial SSTA in 1997 suggest an El Niño/Southern Oscillation (ENSO) influence in the GOA and EBS. The warming in the Bering Sea and North Pacific during summer 1997 appears to be due in part to the confluence of three meteorological factors which favoured clear skies. There was not only an El Niño influence, but also a decadal trend toward higher 700 mb geopotential heights and a particularly strong blocking ridge weather pattern over the Gulf of Alaska in May.

*Correspondence. e-mail: overland@pmel.noaa.gov
Received 15 March 1999
Revised version accepted 25 June 1999

INTRODUCTION

A major warming occurred in the eastern Bering Sea (EBS) during summer 1997, as noted in other papers in this issue (Napp and Hunt, 2001). The intent of this paper is to investigate whether the observed anomalies in the EBS occurred over a larger region and to investigate the relationship of the sea surface temperature anomalies (SSTA) to concurrent meteorological anomalies. Our hypotheses are that the observed oceanographic anomalies in the EBS were influenced, at least in part, by large-scale atmospheric processes, and that these processes have a connection to El Niño/Southern Oscillation (ENSO).

Most studies of North Pacific weather and climate variability concentrate on winter months (Hurrell, 1996; Mantua *et al.*, 1997), but from the fisheries standpoint, solar heating and wind mixing in the spring months April and May are crucial for primary productivity. Sustained temperature anomalies during the summer also influence higher trophic levels. As we shall investigate, the spring and summer have their own modes of atmospheric variability. In winter, low-level air temperature anomalies at mid- and subarctic latitudes over the ocean are associated with temperature advection. In spring and summer, direct heating from insolation contributes substantially to SSTA.

The EBS is remote from tropical influences by direct oceanographic connection; however, indirect connections exist through the atmosphere. Teleconnections between tropical SSTA and the midlatitude atmosphere have been considered primarily during the winter because that is when the atmospheric structure is most suitable for poleward propagation of Rossby waves. Recent studies suggest that there can be a midlatitude response to tropical SSTA in all seasons (Livezey *et al.*, 1997; Trenberth *et al.*, 1998). Because the midlatitude background circulation differs between winter and summer, the nature of the midlatitude response to ENSO also varies seasonally. The spring/summer influence of ENSO at midlatitudes is believed to be related to an equatorward extension of the midlatitude Pacific jet stream and changes in mean flow/eddy feedback (Higgins and Mo, 1997; Straus and Shukla, 1997).

The intrinsic variability of the midlatitude circulation is substantial on time scales of days to decades; it often dominates tropical influences. Nevertheless, based on North Pacific atmospheric anomalies observed during past ENSO events, it appears that the anomalous conditions that occurred in the Gulf of Alaska (GOA) and EBS during April to August 1997 are partially attributed to an atmospheric connection with ENSO. In the next section we show regional anomaly fields for spring and summer, 1997. This is followed by a comparison of 1997 with composite atmospheric fields during previous ENSOs and a summary discussion. Although much discussion is on a plausible ENSO connection, we conclude that the 1997 SST warming is due to a conjunction of an atmospheric decadal trend, a possible ENSO connection, and a particularly strong synoptic weather pattern in May.

ANOMALY FIELDS IN 1997

Sea surface temperature

Monthly SSTA fields in the North Pacific for March to August 1997 are shown in Fig. 1. The fields are taken from the National Centers for Environmental Prediction (NCEP) Reynolds analyses, which are based on a blending of satellite observations and *in situ* data (Reynolds and Smith, 1995). Positive (negative) anomalies equal to or greater than 1° are drawn in shades of red (blue), with a contour interval of 1°C. The onset and intensification of the warm equatorial SSTA associated with El Niño are recognizable, with a 1°C positive anomaly near 180° in April and a large warm signal from May onward. In the EBS in March, the SSTA are −2°C. In April and May, the cold SSTA gradually gave way to the warm anomalies extending westward from the GOA. May also shows the strongest warm SSTA off the west coast of North America at subtropical latitudes. By June, strong warm SSTA stretch from the Equator along the west coast, across the GOA, and into the Bering Sea, persisting through August. The warm SSTA in the EBS in July and August are greater than 2°C. Based on the Reynolds analyses, the EBS showed remarkable SST warming of more than 12°C in a 5 month period, compared with a more typical value of 8°C. In the central North Pacific there is a negative SSTA throughout March–August. The relationship and spatial scales of the positive and negative SSTA are consistent with analysis of historical data (Tanimoto *et al.*, 1997). By November (not shown) the warm SSTA in the Bering Sea and noncoastal North Pacific had dissipated.

700 mb geopotential height

The meteorological fields are from the NCEP/NCAR reanalysis project (Kalnay *et al.*, 1996). The reanalysis project took all available historical observations and a modern atmospheric model for dynamic interpolation and combined these to produce consistent meteorological fields. All anomalies are computed relative to a climatology based on the period 1957–1997. The monthly 700 mb geopotential height anomalies for March to August 1997 for the North Pacific are shown in Fig. 2, which depicts the broad-scale evolution of the tropospheric anomalies that are closely linked to the tangible weather at the surface. March 1997 (Fig. 2a) featured a mostly positive height anomaly over the North Pacific; the anomalous wind flow from the north over the EBS (winds blow parallel to height contours) was associated with relatively strong cold-air advection. Positive height anomalies remained over the northern Bering Sea and western Alaska through April 1997 (Fig. 2b), while prominent negative height anomalies developed over the central Pacific south of 55°N. Lower heights persisted over the Pacific south of 50°N from May to August (Fig. 2c–f). Positive anomalies were centred near the Alaska peninsula in May and August, in western Alaska in June, and were largely absent in July. Generally speaking, during April to August positive 700 mb height anomalies and an anomalous flow from the east off continental Alaska occurred over the EBS.

Of particular importance are the large anomalies that occurred in May (Fig. 2c). The large positive anomalies to the north over the GOA and EBS and negative anomalies to the south in the eastern Pacific constitute a pattern called a blocking ridge (Rex, 1950). The strength and persistence of this pattern during May 1997 largely kept weather systems from propagating over the EBS and Alaska.

Atmospheric variables over the EBS

In this section we discuss atmospheric variables of direct relevance to the EBS. Each figure shows a spatial average for April–August 1997 and a time series for a single point at 57°N, 164°W. This is the location of Mooring 2, the source of much of the ocean profile information presented by Stabeno *et al.* (2001). The 925 mb air-temperature anomalies for April–August 1997 are shown in Fig. 3. The 5 month mean anomaly chart (top panel, Fig. 3a) shows spatial continuity of a large warm anomaly (> 1.5°C) across Alaska and the Bering Sea. We chose the 925 mb level (∼ 800 m above the surface) because it reflects atmospheric boundary layer temperatures, yet avoids localized

Figure 1. Monthly SST anomalies (SSTA) for the North Pacific for 1997. Positive (negative) anomalies equal to or greater than 1°C are drawn in shades of red (blue) with a contour interval of 1°C. Data are from NCEP analysis (Reynolds and Smith, 1995) and are a blend of satellite and *in situ* observations. Note the increase of the equatorial SST anomaly after April. Subarctic SSTA increase after May, first in the Gulf of Alaska and then in the Bering Sea.

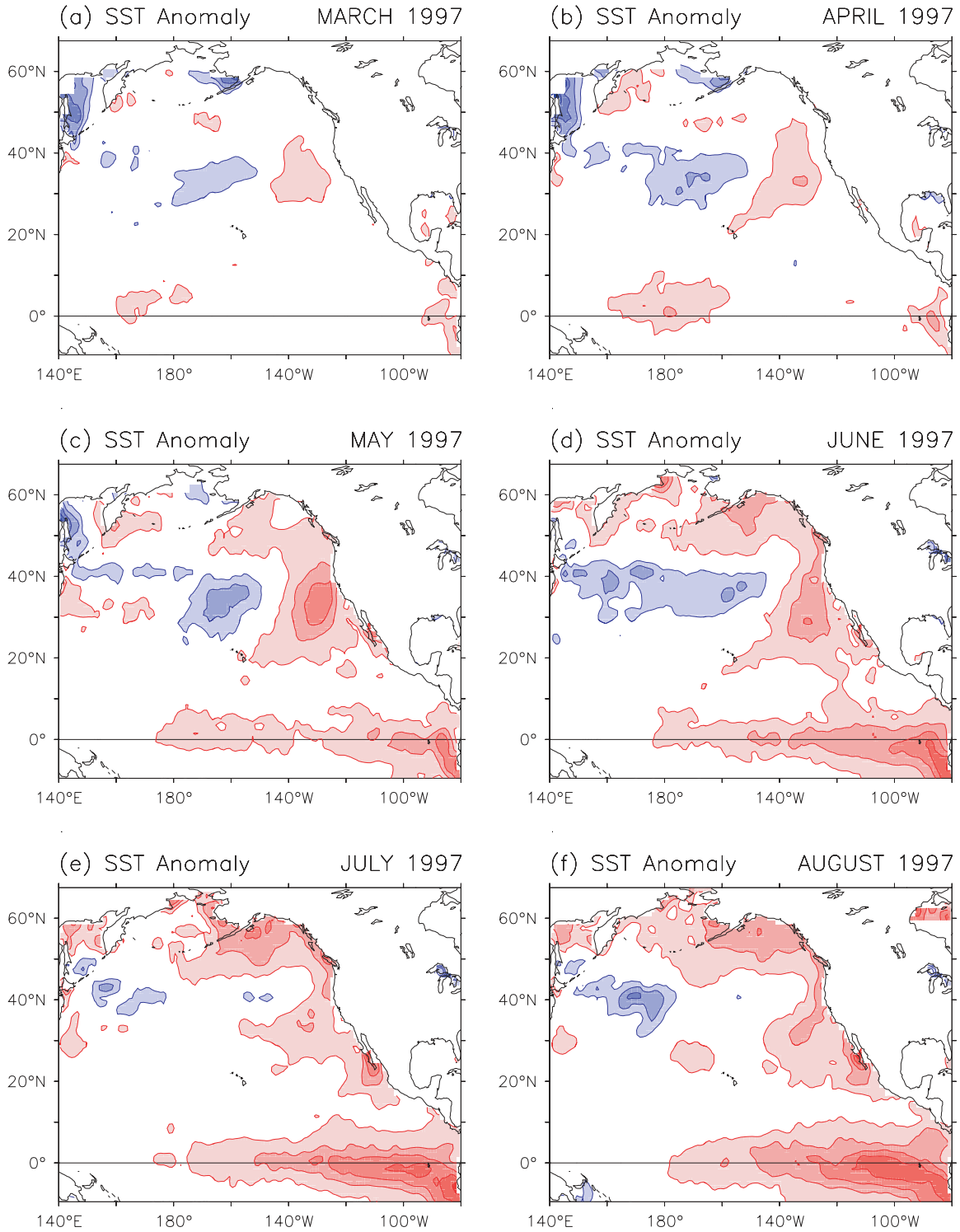

Figure 2. Monthly geopotential height anomalies in metres at 700 mb for March to August 1997. Note changes in contour interval in (e) and (f).

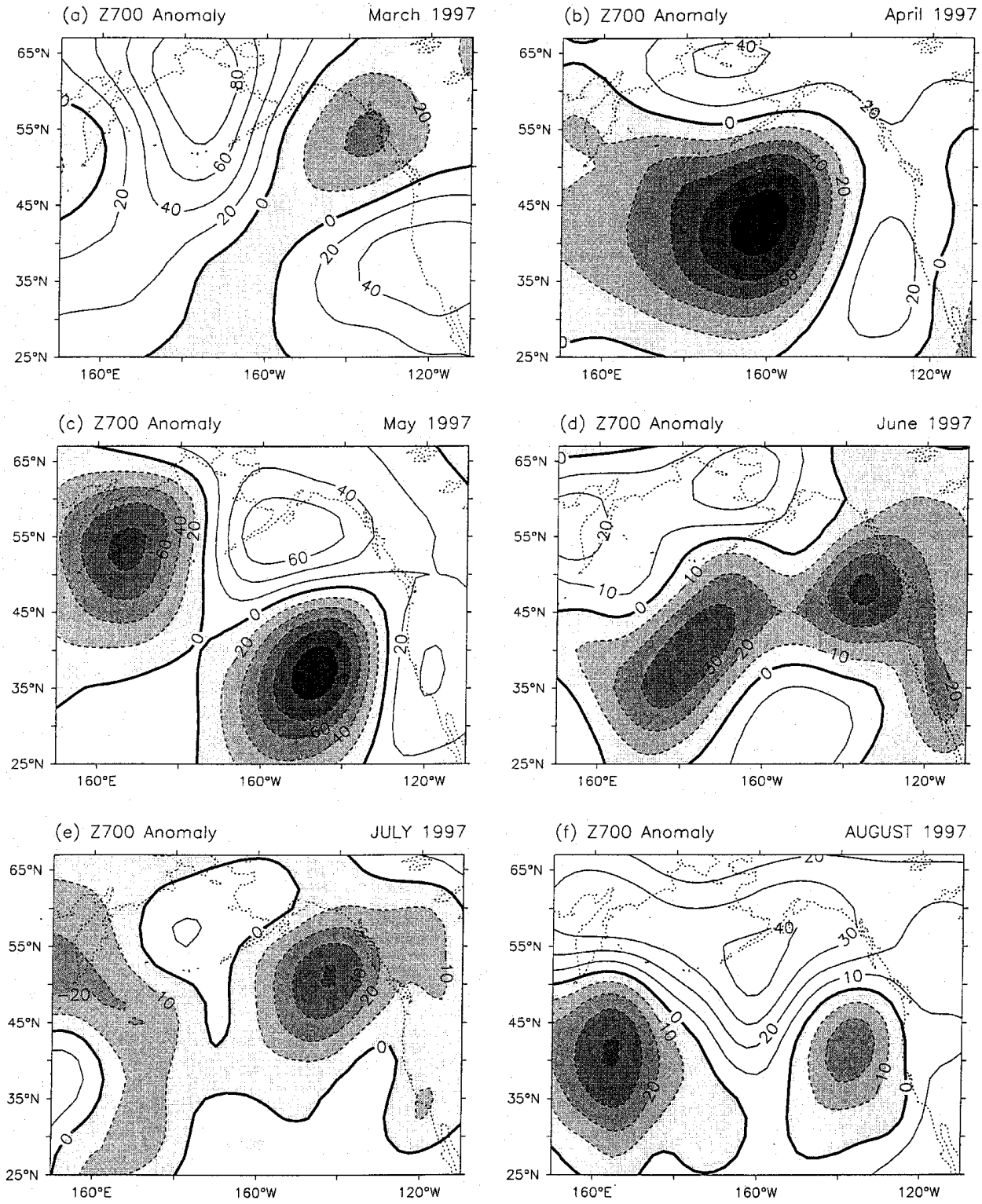

Figure 3. Air temperature anomalies in °C at the 925 mb level for spring and summer of 1997. (a) Five-month (April–August) mean anomaly. (b) Time series of daily anomalies at 57°N, 164°W for the same 5 month period, smoothed with a 5 day running mean. Note the anomalies are consistently positive.

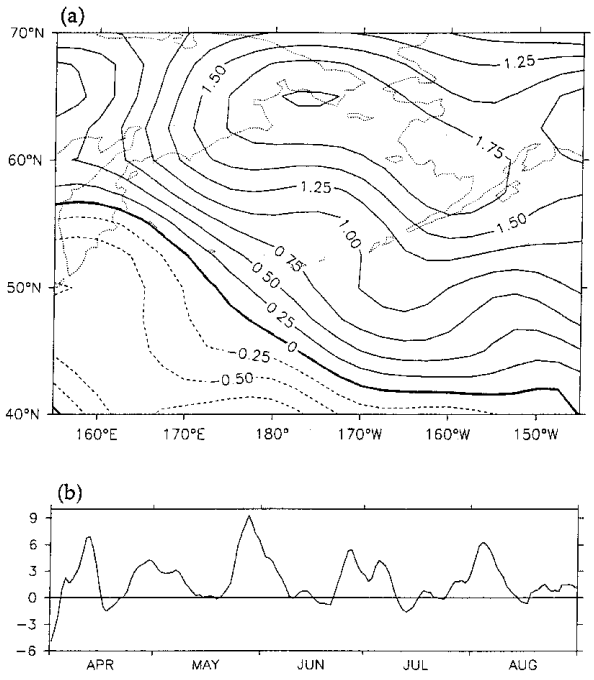

Figure 4. Geopotential height anomalies in metres at 700 mb for spring and summer of 1997. (a) Five-month (April–August) mean anomaly. (b) Time series of daily anomalies at 57°N, 164°W for the same 5 month period, smoothed with a 5 day running mean. There are seven peaks of high geopotential height.

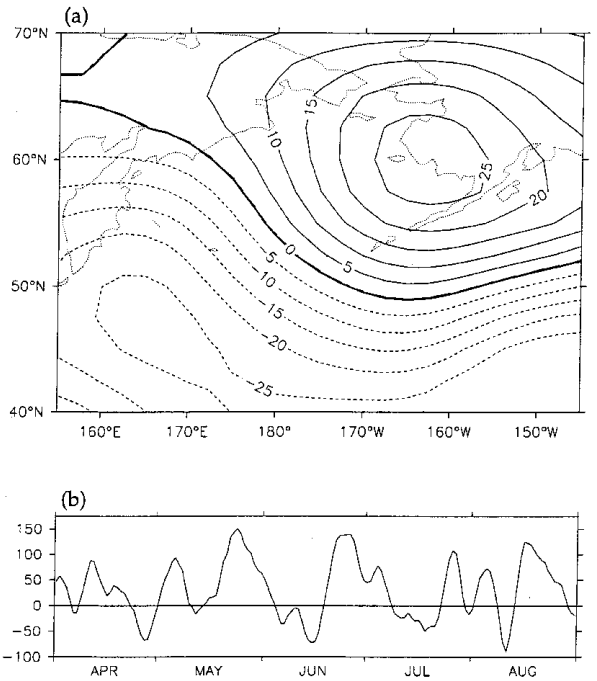

surface influences. The lower panel (Fig. 3b), the time series of the daily 925 mb temperature anomalies at 57°N, 164°W smoothed with a 5 day running mean, shows that EBS temperatures were systematically warm from April to August. There were five maxima of > 3°C; these warm periods typically lasted about 2 weeks.

The 700 mb geopotential height anomalies for April–August are shown in Fig. 4. The 700 mb level is commonly used to illustrate the large-scale atmospheric circulation. As anticipated from Fig. 2, the 5 month mean anomaly pattern shows positive heights over western Alaska and the EBS and negative heights across the Pacific centred at about 45°N. The 700 mb height (Fig. 4b) at the Mooring 2 site also shows the strong tendency for higher geopotential heights in the EBS; particularly prominent positive anomalies occurred in late May, late June, and mid–late August.

In general, clear skies accompany higher 700 mb geopotential heights. One proxy for cloudiness is low-level relative humidity (RH). The 925 mb RH anomaly (Fig. 5a) for April–August 1997, given in per cent, was negative over Alaska and the EBS. Lower RH implies reduced low cloud amounts and increased insolation at the surface. There is an east–west gradient in RH over the Bering Sea, which helps explain the larger positive SST anomalies in the EBS and GOA compared with the western Bering Sea. The time series of daily RH anomalies show extreme dry periods in mid-April, late May, and late June for the EBS. The late May anomaly of −45% is particularly striking compared with the usual daily to weekly variability. Figures 4(a) and 5(a) show the atmospheric boundary layer was relatively dry where anomalous flow was offshore (northerly) and relatively moist where the anomalous flow was onshore (southerly).

Also of interest are the total cloud amount and the net short wave flux at the surface. In the NCEP reanalysis the temperature, geopotential height, and RH fields are dynamic interpolations of observed data into meteorological fields. Cloud amount and radiative fluxes are model-derived parameters. The total cloud amount field (not shown) is similar to the 925 mb RH field. There is less than 57% total cloud north of 56°N and east of 170°W for the April–August composite, which represents an anomaly of ∼ −5%. The net short wave anomalies at the surface for April–August 1997 are shown in Fig. 6. In the 5-month mean, an extra 5–10 W m^{-2} was available to warm the ocean in the

Figure 5. Relative humidity anomalies in percentages at 925 mb for spring and summer of 1997. (a) Five-month (April–August) mean anomaly. (b) Time series of daily anomalies at 57°N, 164°W for the same 5 month period, smoothed with a 5 day running mean.

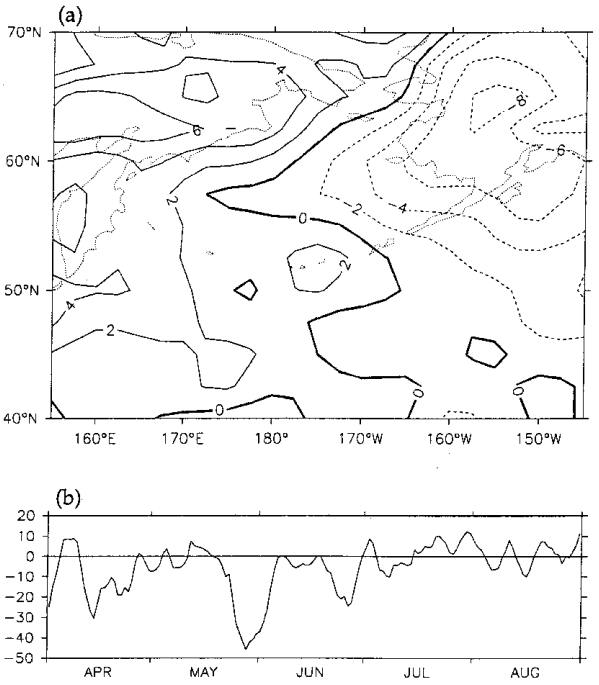

central and eastern Bering Sea, with the greatest anomalous heating over Bristol Bay. The time series in Fig. 6(b) shows that the positive flux anomalies at the Mooring 2 site were about 30 W m^{-2} from mid-May to mid-July. Assuming a typical mixed layer depth of 20 m, this amount of anomalous heat would increase the SST by 2°C. Anomaly values of 10 W m^{-2} and 30 W m^{-2} are greater than one standard deviation for 5-month and 1-month values of solar radiation.

In summary, for the 1997 spring–summer period, there were anomalously high geopotential heights, low RH, increased insolation, and warm low-level temperatures over the EBS. The RH field in particular shows an east–west gradient across the Bering Sea, with drier conditions in the east. Notable coincident peaks in magnitudes of these anomalies occurred in mid-April, late May, and late June. Anomalous solar heating was particularly strong from mid-May to mid-July. In addition to the seasonal anomalies, May had a particularly strong blocking ridge situation over the North Pacific and Bering Sea. It bears emphasizing that intraseasonal fluctuations, of which late May is a prime example, are generally attributable to the inherent extratropical variability of the atmosphere.

Figure 6. Net shortwave radiative flux anomalies at the surface in W m^{-2} for spring and summer of 1997. Positive values of anomalies in (a) and (b) represent increased radiative flux into the ocean, implying a surface warming. (a) Five-month (April–August) mean anomaly. (b) Time series of daily anomalies at 57°N, 164°W for the same 5 month period, smoothed with a 5 day running mean. There is anomalous heating centred on the EBS from late May to early June.

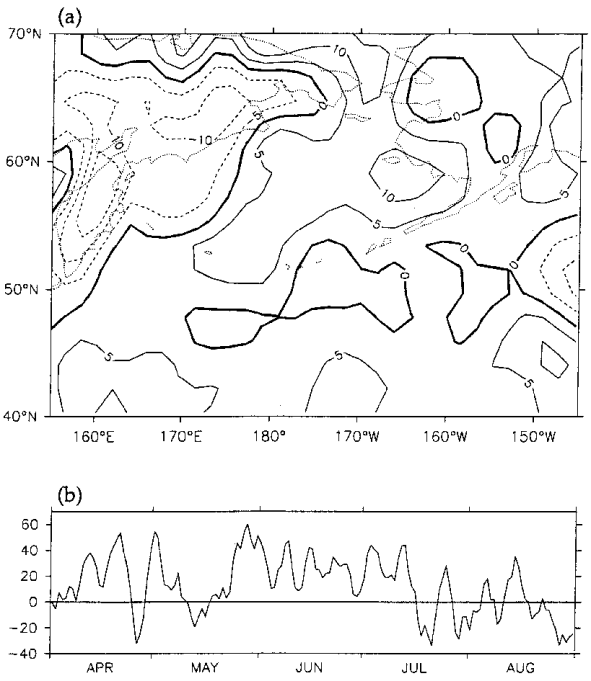

LINK TO THE TROPICAL PACIFIC?

Historical composites

In this section, we examine covariability between equatorial SSTA and midlatitude atmospheric circulation in all spring/summer months with a strong El Niño signal. This is reasonable because the midlatitude atmospheric circulation responds relatively quickly, on time scales of a few weeks or less, to tropical Pacific anomalies (Higgins and Mo, 1997); Livezey *et al.* (1997) took a similar approach. As a measure of equatorial SSTA, we use the NINO3 index for SSTA between 5°N and 5°S and 150–90°W, available from NCEP. Table 1 shows the years with a strong warm signal when the NINO3 indicator was greater than 1.3. The range of years considered is 1958–1996, limited by the NCEP reanalyses data set. A cutoff of 1.3 was used to exclude weaker ENSO events. The composite 700 mb height anomaly maps in Fig. 7 were created from the months selected in Table 1.

Table 1. Years and months when the equatorial SST anomaly index, NINO3, was > 1.3.

March	April	May	June	July	August
1983	1983	1983	1982	1965	1965
1987	1992	1987	1983	1972	1972
1992		1992	1987	1983	1982
		1993		1987	1987

The composite 700 mb geopotential height anomaly chart for March (Fig. 7a) shows a strong negative height anomaly in the central North Pacific, i.e. a deeper Aleutian low. The tendency for a deeper Aleutian low ends abruptly in early spring. The April and May composites show positive height anomalies extending from Canada, across the GOA and into the Bering Sea. This orientation of a positive height anomaly poleward of a negative anomaly (Fig. 7b,c) indicates a 'splitting', of the jet stream or in extreme cases, 'blocking' of the tropospheric flow in the central and eastern Pacific. The composite circulation anomalies undergo another shift in late spring; the June anomaly map (Fig. 7d) is dominated by negative values north of about 45°N extending from the Bering Sea across the entire North Pacific. But this northward shift of the negative height anomalies is temporary. By July and August (Fig. 7e,f), anomalously high heights again are established over the EBS, Alaska, and north-western Canada, and anomalously low heights are present over the Pacific south of about 50°N, especially west of ~ 160°W. Figure 7 suggests that during ENSO events, June represents a transition period between a spring circulation anomaly regime and a summer regime. Because so few years were available for these composites, it is unknown whether the composite anomalies found for June represent a true, systematic shift in the midlatitude response due to ENSO, or whether they merely reflect sampling limitations.

The 700 mb height anomalies in Fig. 7 can be compared directly with the results of Livezey *et al.* (1997). Their results, which include weaker ENSO events, are similar to ours, with a pattern of high over low 700 mb geopotential height anomalies concentrated in the eastern North Pacific in April and May, negative anomalies centred over the Alaska Peninsula in June, and a return to high over low anomalies in the central and western North Pacific in July and August. The analyses of Livezey *et al.* (1997) also included general circulation model (GCM) experiments forced by equatorial SST anomalies. They found similar high-latitude 700 mb patterns as their data analyses, but the pattern amplitudes were greater with the GCM.

Comparison with Spring–Summer 1997

We now compare the composites from previous ENSO forcing shown in Fig. 7 with the individual monthly maps from 1997 (Fig. 2). To facilitate this comparison, we consider the sense and magnitude of the primary atmospheric 'teleconnection' modes for the North Pacific during 1997 as compared with those during previous El Niños. These modes represent the basic building blocks that comprise large-scale atmospheric variability; they form a basis set, and a small number of these modes generally explains a large fraction of the atmospheric variance. The modes of variability provide a compact way to summarize the salient aspects of anomalies in the atmospheric circulation on time scales of a month and longer. The particular modes considered here are calculated and made available by NCEP using rotated principal component analysis (RPCA; Barnston and Livezey, 1987; Bell and Halpert, 1995). The systematic effect of El Niño on wintertime modes has received considerable study (Lau, 1997), but its effect on spring and summer has received less attention.

Summary statistics for the modes germane to the North Pacific are provided in Table 2. Four modes are briefly summarized in terms of their positive phase: (1) the Pacific–North America pattern or PNA, which includes a negative height anomaly in the central North Pacific near 40°N, 160°W and a positive height anomaly centred over western North America; (2) the West Pacific Oscillation (WP), which is a north/south dipole pattern consisting of a negative centre over the Kamchatka Peninsula and a broad positive centre extending from eastern Asia to the dateline along about 30°N; (3) the North Pacific (NP) mode, which consists of a negative centre across the western and central Pacific along about 40°N and a weaker positive centre from eastern Siberia across Alaska to the intermountain region of North America; and (4) the East Pacific (EP) mode, which is a dipole featuring a negative centre over Alaska and western Canada and a positive centre near or east of Hawaii. The PNA and WP tend to contribute more to the variance of the atmospheric circulation from autumn into early spring; the NP and EP tend to contribute largely from spring to midsummer. A complete description of these modes, including maps of their spatial patterns and time series of their amplitudes, is available at http://www.cpc.noaa.gov/data/teledoc/teleconnections.html.

The 1997 and El Niño composite 700 mb height anomaly maps for March (Figs 2a and 7a, respectively) are dissimilar. The 1997 El Niño was only beginning to develop in March. The differences between

Figure 7. Monthly composite 700 mb geopotential height anomaly maps for years when there is a large positive equatorial SSTA, NINO3 > 1.3. See Table 1 for the months that form each composite.

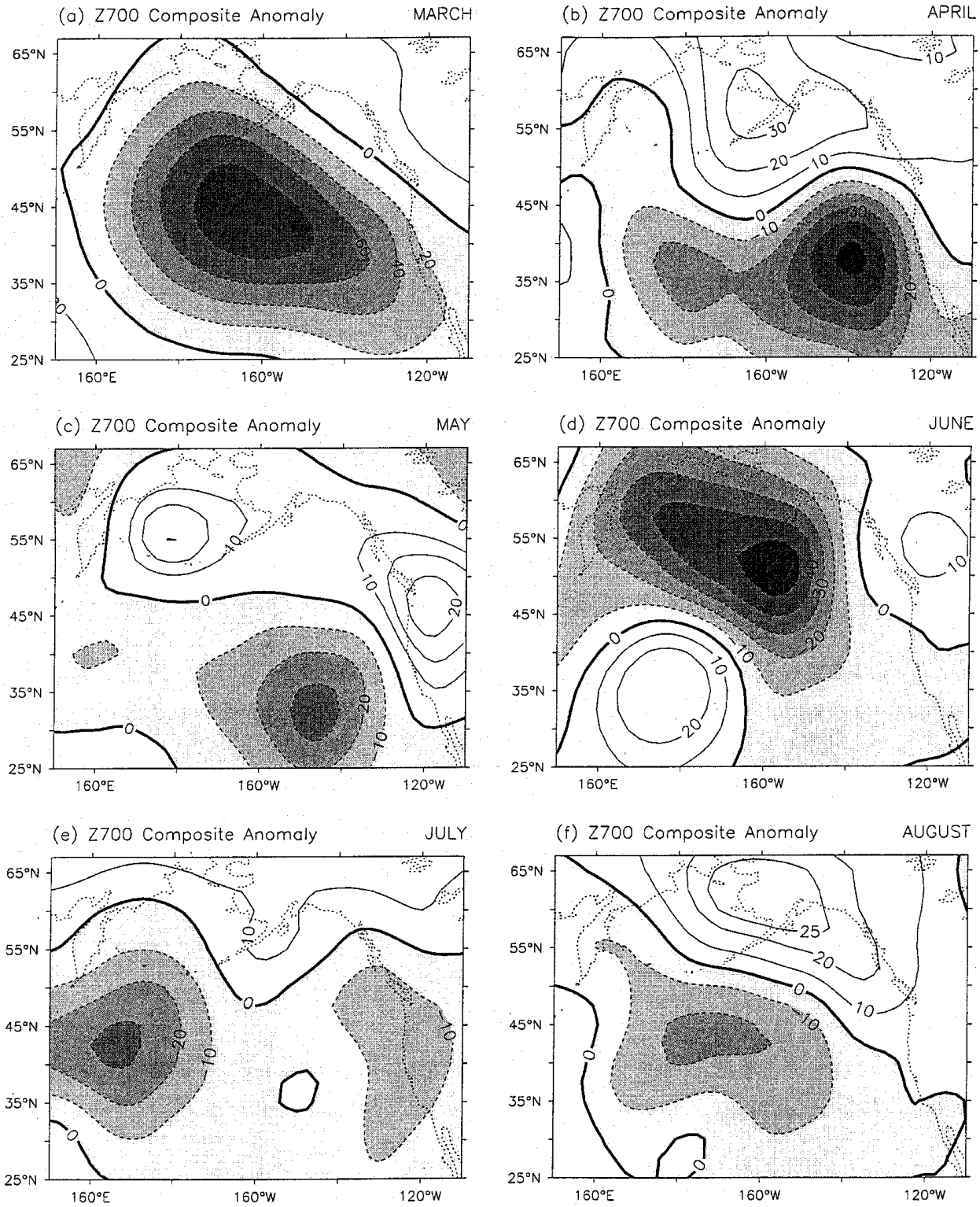

Table 2. Standardized amplitude of various teleconnection modes during 1997 and for the composite El Niño. See text for details.

Mode	March	April	May	June	July	August	April–August
PNA 1997	−0.9	0.1	−1.5	—	—	−0.4	−0.36
Composite	1.5	0.0	−0.8	—	—	−0.8	
WP 1997	0.0	0.3	0.5	−1.2	−0.2	0.0	−0.11
Composite	0.9	−0.2	0.7	0.1	0.0	0.7	
NP 1997	0.5	1.7	1.6	0.5	0.4	—	0.80
Composite	0.2	0.3	0.4	0.3	1.2	—	
EP 1997	0.0	−1.7	−1.6	−0.8	0.4	—	−0.74
Composite	−1.5	−1.8	−1.0	0.5	0.0	—	

Figs 2(a) and 7(a) in large part reflect differences in the sense of the PNA pattern. By April 1997 positive SSTA became prominent near the dateline in the equatorial Pacific, and the 700 mb height anomalies (Fig. 2b) began to resemble the El Niño composite (Fig. 7b), particularly in the tendency for splitting the atmospheric westerly flow in the western North Pacific. Much of this agreement can be attributed to the strong negative phase of the EP and positive phase in the NP in both April 1997 and the April composite (Table 2). This correspondence continued through May, where the anomalies for 1997 (Fig. 2c) are an amplified version of the May composite (Fig. 7c). As shown in Table 2, the PNA, NP, and EP all had greater amplitudes and the same sign in May 1997 as in the May composite. The location of the centres of action of the NP imply that it had an especially prominent role in the anomalous atmospheric conditions for the EBS. The resemblance between 1997 and the composite for June was weak; positive 700 mb geopotential height anomalies persisted over the Bering Sea and western Alaska in 1997 (Fig. 2d) while previous El Niños tended to include negative anomalies in that region (Fig. 7d). Better correspondence is found for July 1997, during which the height anomalies over the Bering Sea and Alaska were small, but negative anomalies were favoured over the Pacific south of 55°N in both 1997 (Fig. 2e) and the composite (Fig. 7e). Finally, August 1997 featured a resumption of significantly higher heights over the Bering Sea and Alaska, with negative anomalies to the south over the North Pacific (Fig. 2f), again representing an amplified version of the composite (Fig. 7f).

We have made estimates of the individual contributions of each of the modes discussed above to the two extrema of the April–August 1997 height anomalies (Table 2, last column). The magnitudes of these extrema were comparable to the sums of the individual contributions from each of the four modes. Thus the modes provided a methodology for comparing 1997 to the ENSO composites.

In summary, the atmospheric circulation for the North Pacific during the months of May and August 1997 best resembled that of previous El Niños. The overall similarity on a seasonal basis is shown in Fig. 8, which compares the April–August mean 700 mb height field for 1997 and El Niño composites. The correspondence is compelling but not incontrovertible, because the El Niño composite is based on relatively few events. The influence of the ENSO on Northern Hemisphere atmospheric conditions is most apparent on a seasonal time scale. This is because the intrinsic variability of the midlatitude atmosphere circulation can obscure such influence on shorter time scales (Trenberth *et al.*, 1998). Even though these linkages tend to be somewhat weaker than during the cool season, the internal variability of the extratropical circulation is also reduced, resulting in small seasonal dependence in the signal-to-noise ratio for ENSO forcing of northern latitudes (Trenberth *et al.*, 1998).

DISCUSSION

As suggested in the previous section, the El Niño of 1997 may have impacted the North Pacific during April and May even though tropical SSTA were only ~ 1°C. These modest anomalies must be considered in light of the seasonal cycle of the tropical Pacific. Because central and eastern tropical Pacific SSTs are warmest during the boreal spring, relatively minor warming can cause the SST to exceed the 27°C threshold for deep cumulus convection (Gadgil *et al.*, 1984). It is these anomalies in deep convection and the associated upper-tropospheric zonal wind anomalies that have repercussions on the global atmospheric circulation. As shown in Table 3, even though the El Niño was only beginning in the spring of 1997 in terms of the SSTA, there were already significant

Figure 8. April–August 700 mb geopotential height fields: (a) composite for months with a strong El Niño signal; (b) April–August 1997.

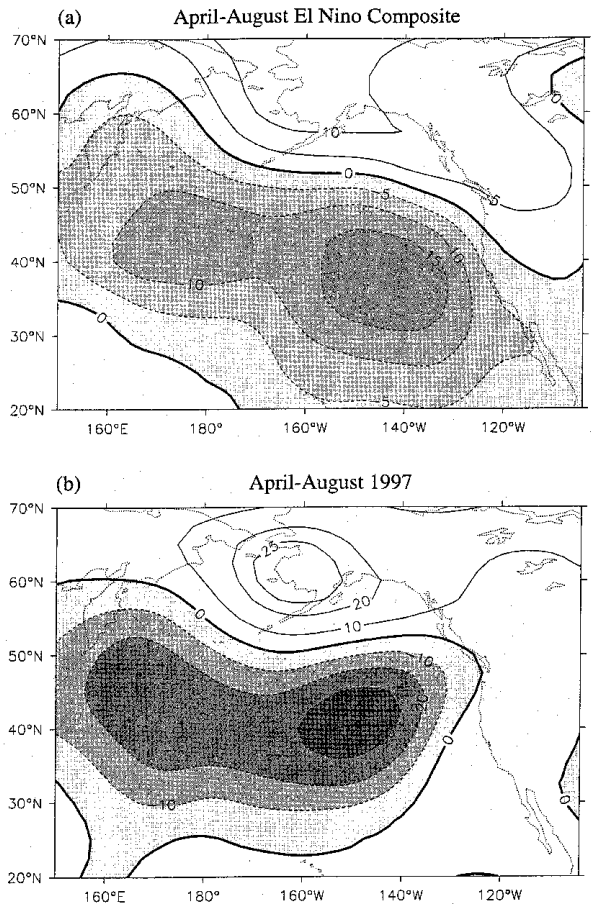

Table 3. Index values for 1997 for the tropical Pacific (from the *Climate Diagnostics Bulletin*).

Month	NINO3	OLR	200 mb Wind Index
March	0.2	−0.7	1.4
April	0.4	−1.1	0.6
May	1.4	−1.7	0.0
June	2.1	−0.9	−1.3
July	2.7	−1.3	−0.8
August	3.1	−1.6	−0.6
September	3.3	−1.2	−0.8

anomalies in the deep convection, as indicated by the outgoing longwave radiation (OLR), and a significant trend in the 200 mb zonal wind anomalies.

The forcing by ENSO during the spring and summer of 1997 needs to be considered in the context of the longer-term variability of the atmosphere over the Pacific and Alaska. There is increasing evidence that significant fluctuations occur in the extra-tropical Pacific's atmosphere–ocean system on decadal time scales. Most of the attention in this regard has focused on winter conditions (e.g. Mantua *et al.*, 1997); here we examine spring/summer conditions. Figure 9 illustrates aspects of the background state of the atmospheric circulation over the North Pacific during April–July from 1950 to the present, using the NP and EP indices. These time series show that the NP and EP tend to be of opposite phase on decadal time scales, which means that these modes reinforce one another in contributing to height anomalies over Alaska and the EBS and anomalies of the opposite phase over the central North Pacific. Notably, the NP (EP) has tended to be positive (negative) in the 1990s. It is unknown whether decadal trends in the North Pacific can be ascribed primarily to the forcing by the tropical Pacific (Zhang *et al.*, 1997), or represent a modified baseline upon which the interannual forcing by the tropical Pacific is exerted.

It should be noted that not all El Niños are associated with a major North Pacific response, termed Niño North (Wooster and Fluharty, 1985). From

Figure 9. Amplitudes of the North Pacific (NP) and East Pacific (EP) teleconnection modes averaged for April to July. Also shown is the amplitude of the NINO3 index for the same period. Both the NP and EP switched phase from the 1980s into the 1990s. Opposite signs of the NP and EP tend to reinforce a similar north–south variation of 700 mb geopotential height anomalies in the GOA. Positive NP values reflect higher geopotential heights over the Bering Sea and lower heights over the central North Pacific.

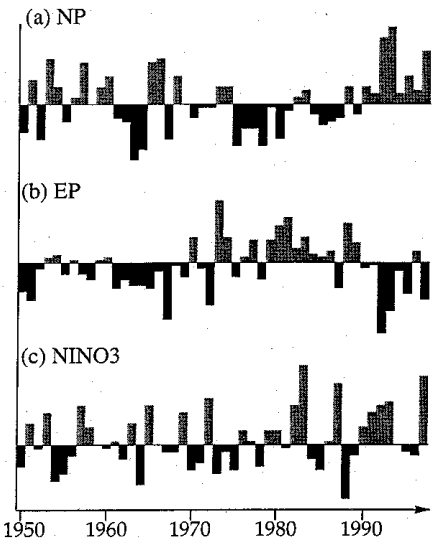

inspection of Fig. 9, there is a correspondence between the NINO3 index and a positive NP pattern in 1957, 1965, 1992, and 1997, but not in 1972 or 1983. Hoerling and Kumar (1997a,b) discuss that natural internal variability of the Northern Hemisphere circulation is often substantial enough to offset the systematic influence of ENSO on midlatitudes.

SUMMARY

The warm SSTA in the EBS and GOA during the spring and summer of 1997 were partly related to concurrent, large-scale atmospheric anomalies. The principal processes involved in producing the warm SSTA were enhanced warm-air advection and insolation, as revealed by the anomalous distributions of low-level temperature, geopotential height, relative humidity, and cloud cover.

A return to normal SST conditions in the EBS and GOA occurred by November 1997. These changes appear to be associated with enhanced storminess accompanying a strong (deep) Aleutian low. A deeper Aleutian low is a typical winter feature of previous ENSOs (Horel and Wallace, 1981).

The atmospheric circulation anomalies for the EBS and GOA during spring and summer of 1997 appear to represent a particularly strong manifestation of the effect of ENSO. Especially in the mean for April to August (Fig. 8), the atmospheric conditions over the North Pacific during 1997 have a striking resemblance in sense and location to those which occurred in a composite from previous strong El Niños. Support for a connection to the tropical Pacific during this time of year is provided by the GCM results of Kuman and Hoerling (1995) and Livezey *et al.* (1997). A particularly prominent role for the tropical Pacific should be expected because local ENSO forcing, i.e. tropical Pacific SST, OLR, and 200 mb zonal wind anomalies during the spring and summer of 1997, were exceptionally large by historical standards.

The warming in the Bering Sea and North Pacific during summer 1997 appears to be due in part to the confluence of three atmospheric factors: a decadal trend toward higher 700 mb geopotential heights as noted in the NP pattern; the atmospheric ENSO connection; and a particularly strong intraseasonal blocking ridge weather pattern in May. These three factors may not be independent. Thus the seasonal ENSO influence was one factor contributing to higher 700 mb geopotential heights and thus warming in the EBS and GOA during summer 1997. The decadal trend creates a situation where ENSO and interannual and intraseasonal atmospheric variability may result in more extreme oceanographic consequences.

ACKNOWLEDGEMENTS

We appreciate the support of the NASA Polar Programs, ONR Polar Programs, and the International Arctic Research Center (IARC), in preparation of this manuscript. We also appreciate Ryan Whitney's careful word processing of the text. This is NOAA/Pacific Marine Environmental Laboratory contribution no. 1967 and Joint Institute for Study of the Atmosphere and Ocean contribution no. 588.

REFERENCES

Barnston, A.G. and Livezey, R.E. (1987) Classification, seasonality and persistence of low-frequency atmospheric circulation patterns. *Mon. Weather Rev.* **115:**1083–1126.

Bell, G.D. and Halpert, M.S. (1995) *Atlas of Intraseasonal and Interannual Variability 1986–1993 (NOAA Atlas no. 12)*. Washington, DC: CPC, NOAA/NWS/NMC, 256 pp.

Bell, G.D. and Janowiak, J.E. (1995) Atmospheric circulation associated with the Midwest floods of 1993. *Bull. Am. Meteor. Soc.* **76:**681–695.

Gadgil, S., Joseph, P.V. and Noshi, N.V. (1984) Ocean–atmosphere coupling over the monsoon regions. *Nature* **312:**141–143.

Higgins, R.W. and Mo, K.C. (1997) Persistent North Pacific Circulation anomalies and the tropical intraseasonal oscillation. *J. Climate* **10:**223–244.

Hoerling, M.P. and Kumar, A. (1997a) Why do North American climate anomalies differ from one El Niño event to another? *Geophys. Res. Lett.* **24:**1059–1062.

Hoerling, M.P. and Kumar, A. (1997b) Origins of extreme climate states during 1982–83 ENSO winter. *J. Climate* **10:**2859–2870.

Horel, J.D. and Walace, J.M. (1981) Planetary scale atmospheric phenomena associated with the southern oscillation. *Mon. Weather Rev.* **109:**813–829.

Hurrell, J.W. (1996) Influence of variations in extratropical wintertime teleconnections on Northern Hemisphere temperature. *Geophys. Res. Lett.* **23:**665–668.

Kalnay, E., Kanamitsu, M. and Kistler, R. *et al.* (1996) The NCEP/NCAR 40-year reanalysis project. *Bull. Am. Meteor. Soc.* **77:**437–471.

Kuman, A. and Hoerling, M.P. (1995) Prospects and limitations of atmospheric GCM climate predictions. *Bull. Am. Meteor. Soc.* **76:**335–345.

Lau, N.C. (1997) Interactions between global SST anomalies and the midlatitude atmospheric circulation. *Bull. Am. Meteor. Soc.* **78:**21–33.

Livezey, R.E., Masutani, M., Leetmaa, A., Rui, H., Ji, M. and Kumar, A. (1997) Teleconnective response of the Pacific–North American region atmosphere to large central Equatorial Pacific SST anomalies. *J. Clim.* **10:**1787–1819.

Mantua, N.J., Hare, S.R., Zhang, Y., Wallace, J.M. and Francis, R.C. (1997) A Pacific interdecadal climate oscillation with impacts on salmon production. *Bull. Am. Meteor. Soc.* **78:**1069–1079.

Napp, J.M. and Hunt, G.L. Jr (2001) Anomalous conditions in the southeastern Bering Sea, 1997: linkages among climate, weather, ocean, and biology. *Fish. Oceanogr.* **10:**61–68.

Rex, D.F. (1950) Blocking action in the middle troposphere and its effects on regional climate, I: an aerological study of blocking. *Tellus* **2:**196–211.

Reynolds, R.W. and Smith, T.M. (1995) A high-resolution global sea surface temperature climatology. *J. Climate* **8:**1571–1583.

Stabeno, P.J., Bond, N.A., Kachel, N.B., Salo, S.A. and Schumacher, J.D. (2001) On the temporal variability over the southeastern Bering Sea. *Fish. Oceanogr.* **10:**81–98.

Straus, D.M. and Shukla, J. (1997) Variations of midlatitude transient dynamics associated with ENSO. *J. Atmos. Sci.* **54:**777–790.

Tanimoto, Y., Iwasaka, N. and Hanawa, K. (1997) Relationships between sea surface temperature, the atmospheric circulation and air–sea fluxes on multiple time scales. *J. Meteor. Soc. Japan* **75:**831–849.

Trenberth, K.E., Branstator, G.W., Karoly, D., Kumar, A., Lau, N. and Ropelewski, C. (1998) Progress during TOGA in understanding and modeling global teleconnections associated with tropical sea surface temperature. *J. Geophys. Res.* **103:**14291–14324.

Wooster, W.S. and Fluharty, D.L. (1985) *El Niño North*. Washington Sea Grant, 312 pp.

Zhang, Y., Wallace, J.M. and Battisti, D.S. (1997) ENSO-like interdecadal variability 1990–93. *J. Clim.* **10:**1004–1020.